Electronic Supplementary Material (ESI) for Physical Chemistry Chemical Physics.

Conformational switching via intramolecular H-bond modulates fluorescence lifetime in a novel coumarin-imidazole conjugate

Indranil Bhattacharjee,[†] Nita Ghosh,[‡] Abhinav Raina[†], Jyotishman Dasgupta,[‡] and Debdas Ray*[,†]

[†]Department of Chemistry, School of Natural Sciences, NH-91, Tehsil Dadri, District Gautam Buddha Nagar, Uttar Pradesh, 201314, India.

[‡]Department of Chemical Sciences, Tata Institute of Fundamental Research, B-127, Mumbai-1, Homi Bhabha Road, 400 005, India.

Table of contents

Synthesis and Characterization	S2
NMR spectroscopy Characterization	S3
Single Crystal X-ray Diffraction (SCXRD) Analysis	S13
Photophysical property	S16
Fluorescence upconversion decay	S17
Fluorescence TCSPC decay	S19
Theoretical Calculations	S21
NBO analysis	S22
Frontier Orbital Analysis	S24
Optimized coordinate	S26
References	S36

Synthesis and characterization

7-diethylamino-3-nitro-chromene-2-one (1a): This compound was synthesized using a modified literature procedure.[S1] 1.25 g (1.0 equiv.), of 4-diethylaminosalicyldehyde, 1.14 mL (1.0 equiv.), of ethylnitroacetate and 0.2 mL of piperidineacetate were taken in a 25 mL ^{n}BuOH and the reaction mixture was allowed to reflux for 12 h. After completion of the reaction (monitored by TLC), it was allowed to settle at room temperature. The precipitate was filtered and washed with ^{n}BuOH (2 × 10 mL) and finally dried in vacuum to afford an orange solid (1.42 g, 86%). ^{1}H NMR (400 MHz in CD_3CN): δ 8.77 (s, 1H), 7.55 (d, *J* = 8.0 Hz, 1H), 6.84 (dd, *J* = 8.0 Hz, 1H), 6.55 (d, *J* = 4.0 Hz, 1H), 3.54 (q, *J* = 8.0 Hz, 4H), 1.22 (t, *J* = 8.0 Hz, 6H) ppm. ^{13}C NMR (100 MHz in CD_3CN) : δ 159.74, 155.79, 154.37, 144.61, 133.77, 112.34, 107.10, 97.18, 46.02, 12.58 ppm.

3-Amino-7-diethylamino-chromene-3-one (1b): In a 100 mL round-bottomed flask $SnCl_2 \bullet 2H_2O$ (4.0 equiv.) and 10 mL of 5 N HCl were taken. To it compound **1a** (1.2 g, equiv.) was added and the solution was stirred at 60 ^{o}C for 5 h. After completion of the reaction, 5 M NaOH solution was added to neutralize the excess acid. The aqueous phase was extracted with ethyl acetate (3 × 10 mL). This organic layer was dried with anhydrous Na_2SO_4 and evaporated to dryness which afforded a pale yellow solid (1 g, 74 %). ^{1}H NMR (400 MHz in $CDCl_3$): δ 7.17 (d, *J* = 8.0 Hz, 1H), 6.97 (s, 1H), 6.60 (d, *J* = 8.0 Hz, 1H), 6.52 (s, 1H), 5.92 (br, 1H), 3.35 (q, *J* = 8.0 Hz, 4H), 1.17 (t, *J* = 8.0 Hz, 6H) ppm. ^{13}C NMR (100 MHz in $CDCl_3$): δ 161.36, 151.97, 148.58, 136.34, 127.41, 116.29, 109.82, 108.82, 98.08, 44.79, 12.58 ppm.

NMR spectroscopy Characterization:

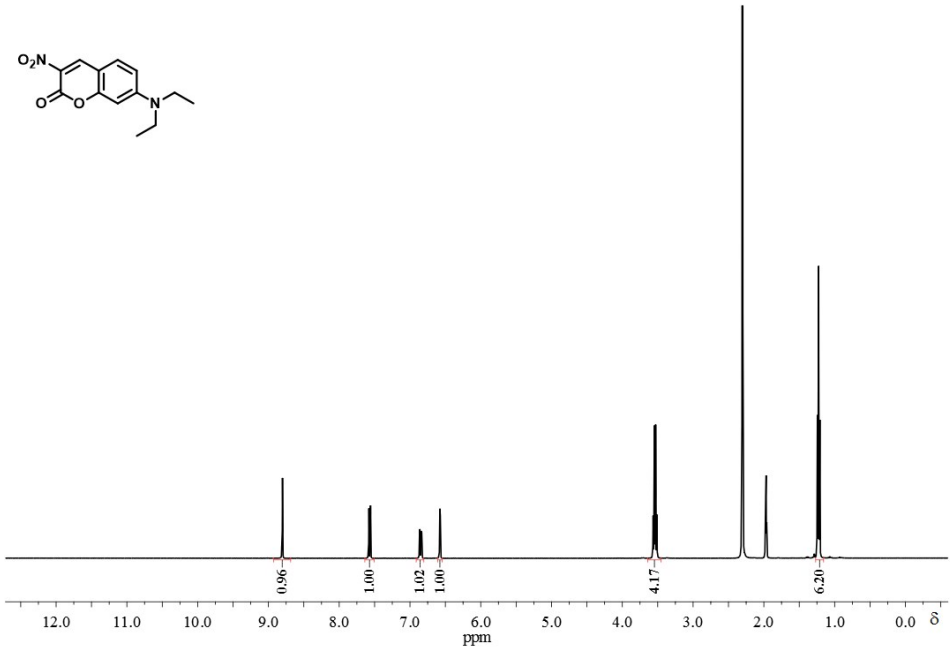

Fig. S1 ^{1}H NMR spectrum (400 MHz, CD_3CN, RT) of **1a**.

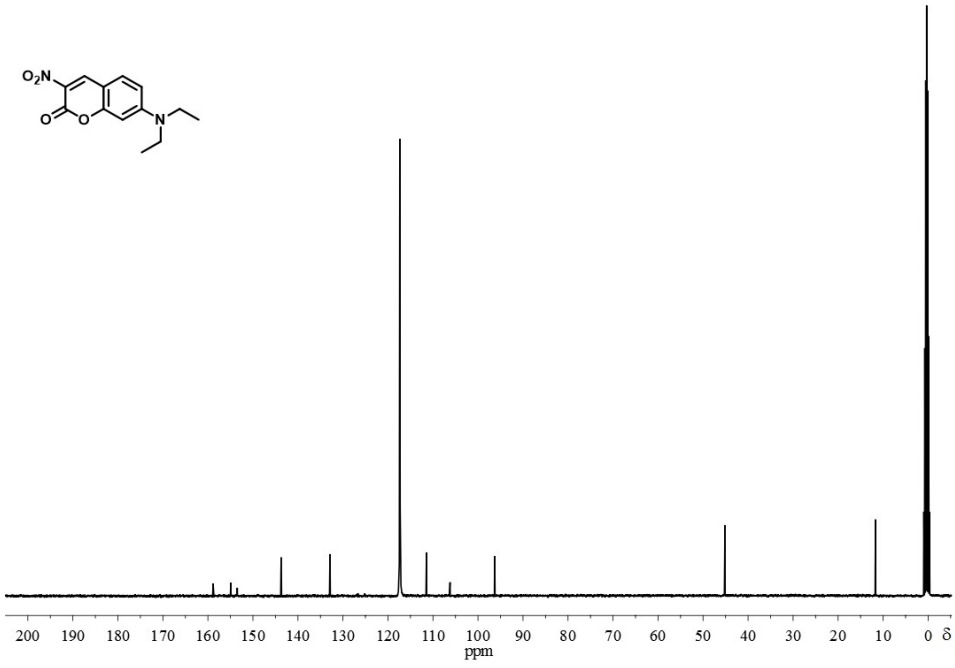

Fig. S2 ^{13}C NMR spectrum (100 MHz, CD_3CN, RT) of **1a**.

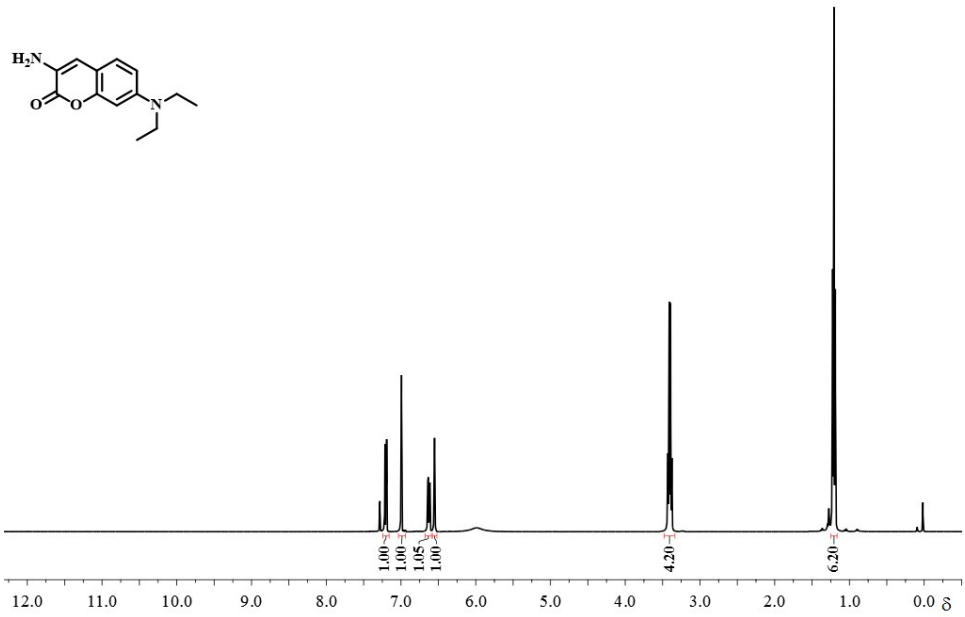

Fig. S3 ^{1}H NMR spectrum (400 MHz, $CDCl_3$, RT) of **1b**.

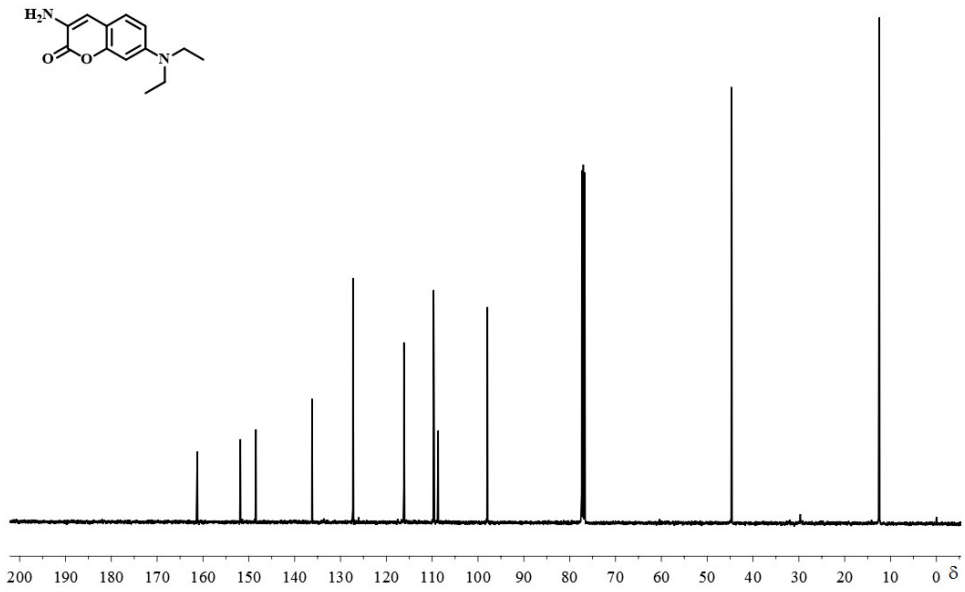

Fig. S4 ^{13}C NMR spectrum (100 MHz, $CDCl_3$, RT) of **1b**.

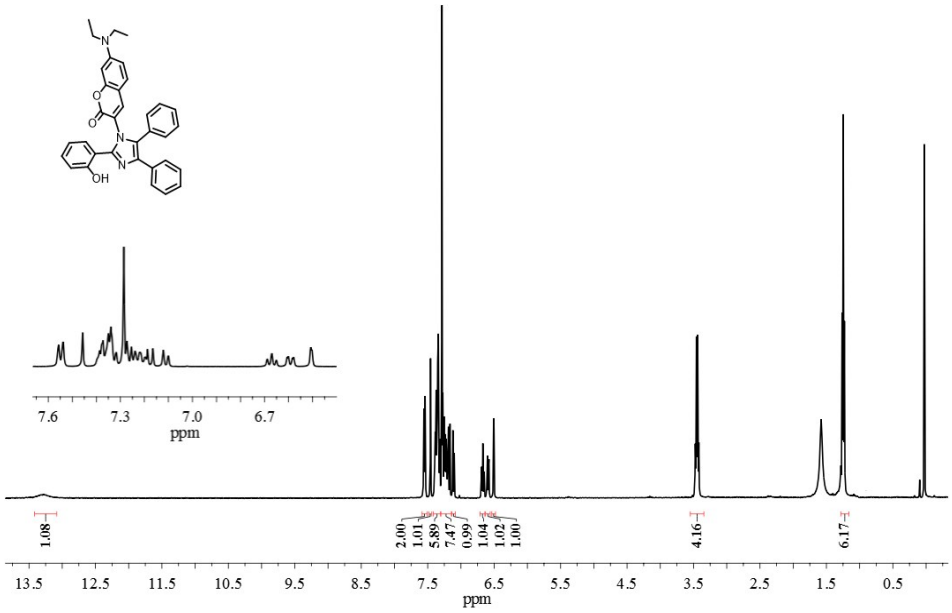

Fig. S5 ^{1}H NMR spectrum (400 MHz, $CDCl_3$, RT) of **1**.

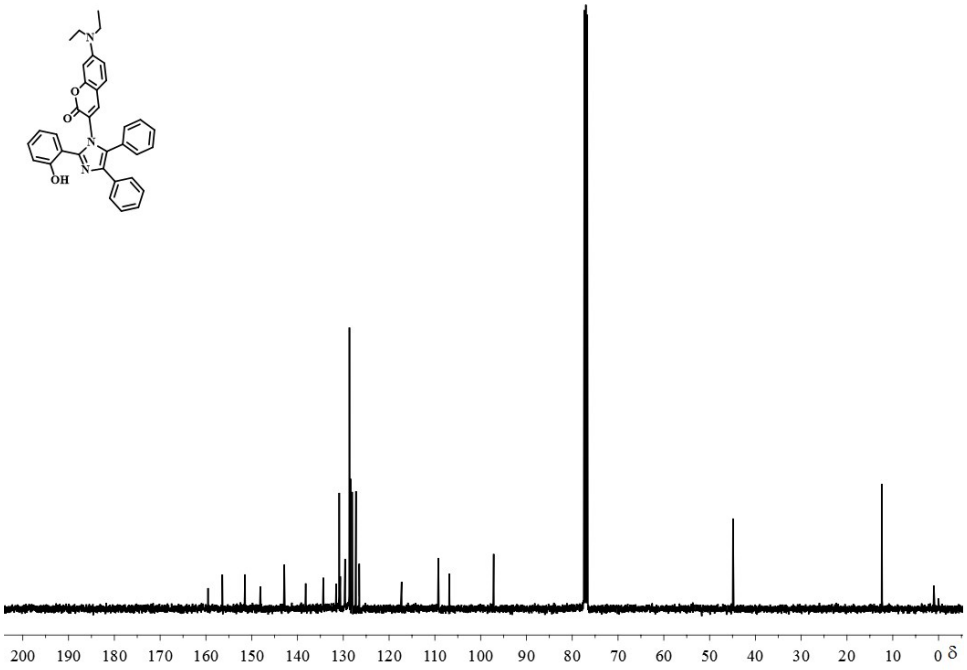

Fig. S6 ^{13}C NMR spectrum (100 MHz, $CDCl_3$, RT) of **1**.

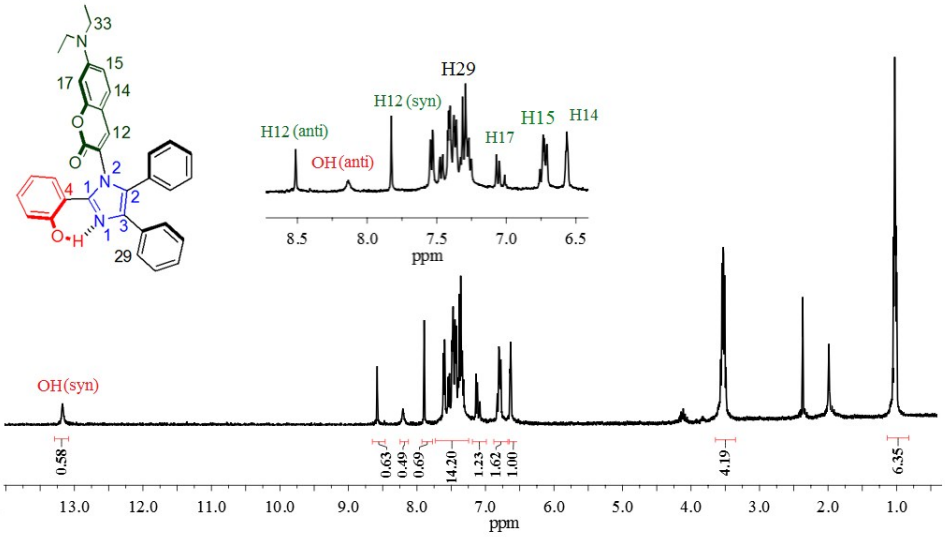

Fig. S7 ^{1}H NMR spectrum (400 MHz, CD_3CN, RT) of compound **1**, with partial peak assignments

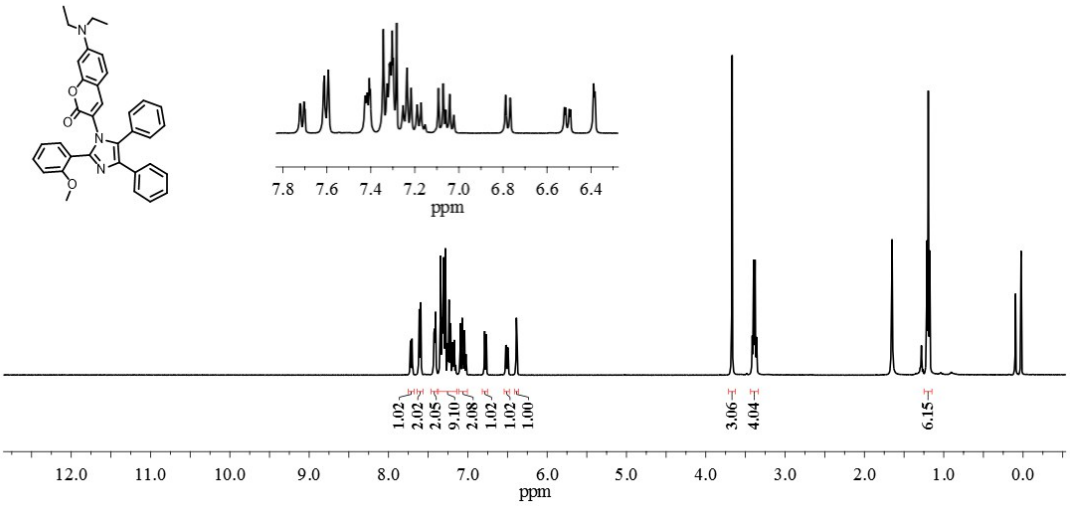

Fig. S8 ^{1}H NMR spectrum (400 MHz, $CDCl_3$, RT) of **2**.

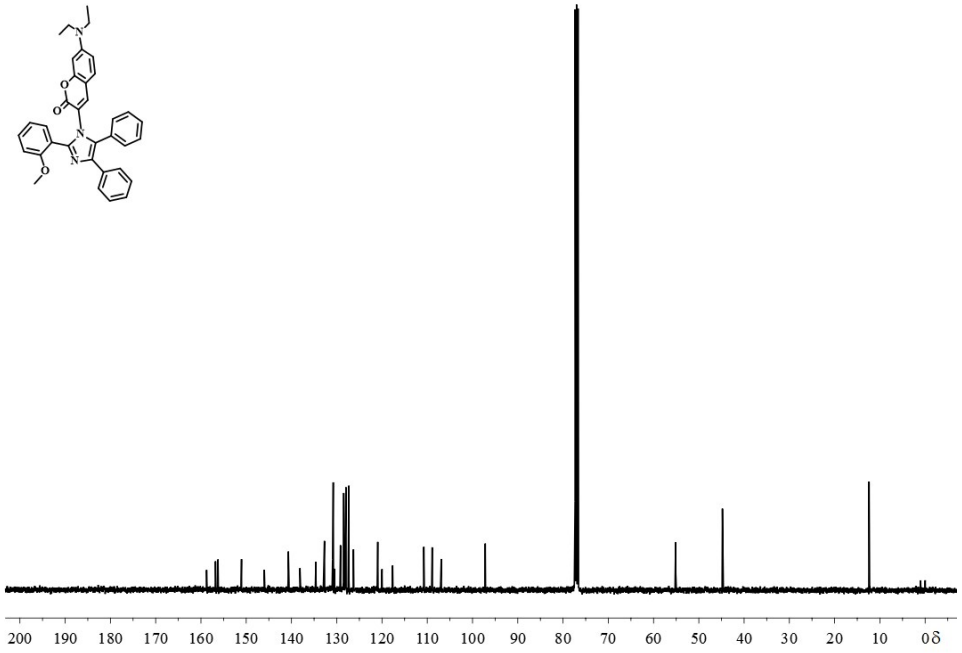

Fig S9 ^{13}C NMR spectrum (100 MHz, $CDCl_3$, RT) of **2**.

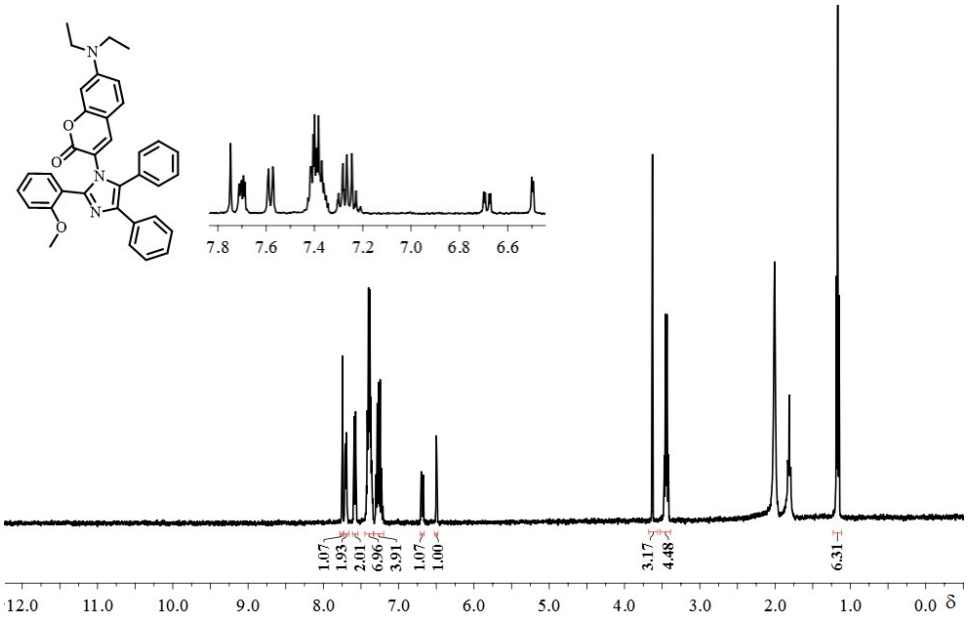

Fig. S10 ^{1}H NMR spectrum (400 MHz, CD_3CN, RT) of **2**.

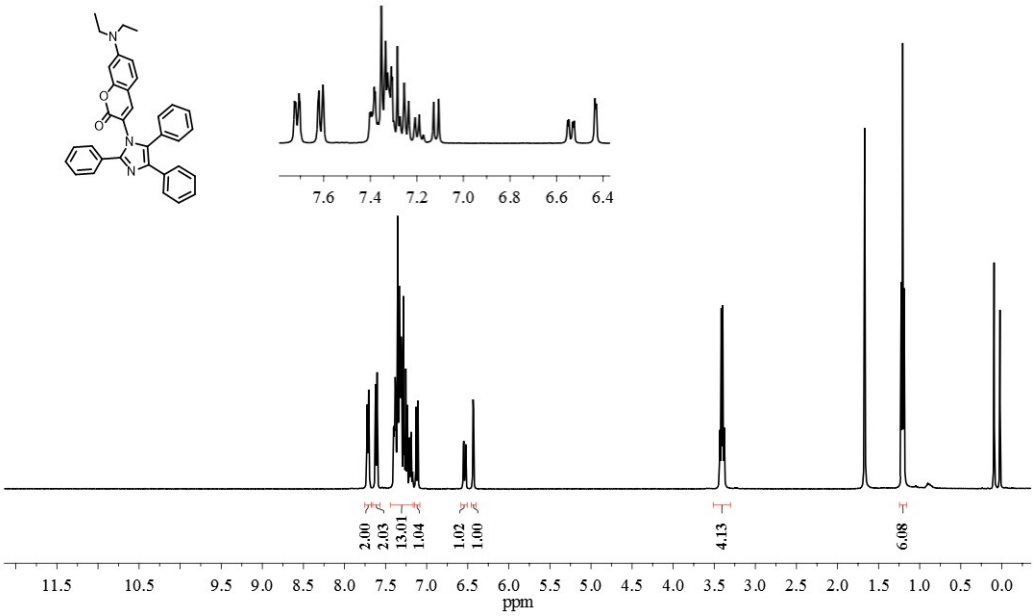

Fig. S11 ^{1}H NMR spectrum (400 MHz, $CDCl_3$, RT) of **3**.

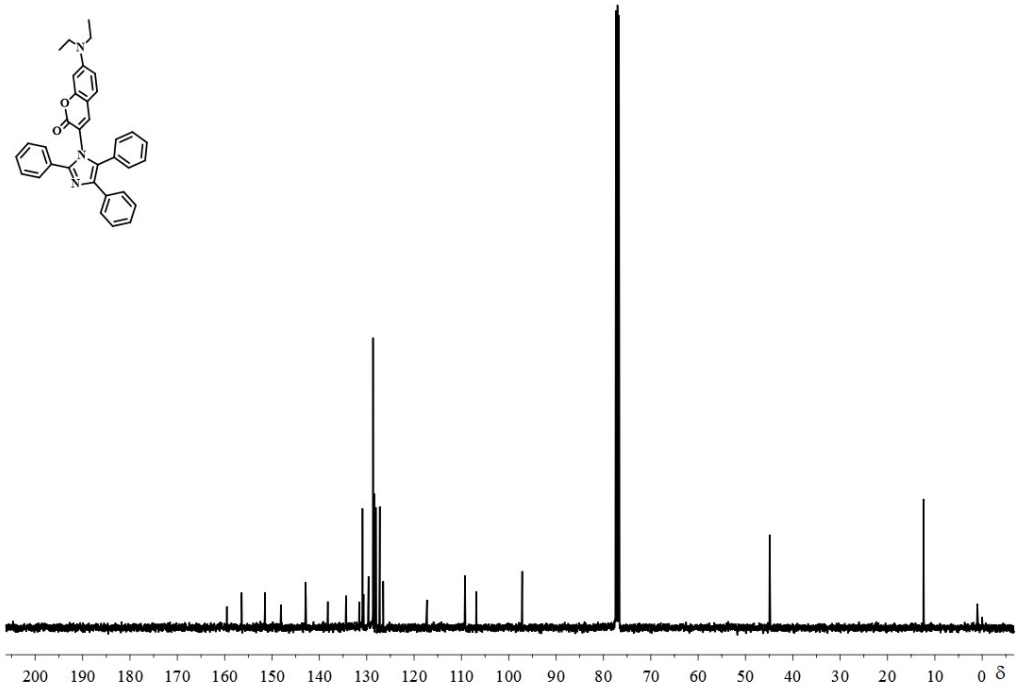

Fig. S12 ^{13}C NMR spectrum (100 MHz, $CDCl_3$, RT) of **3**.

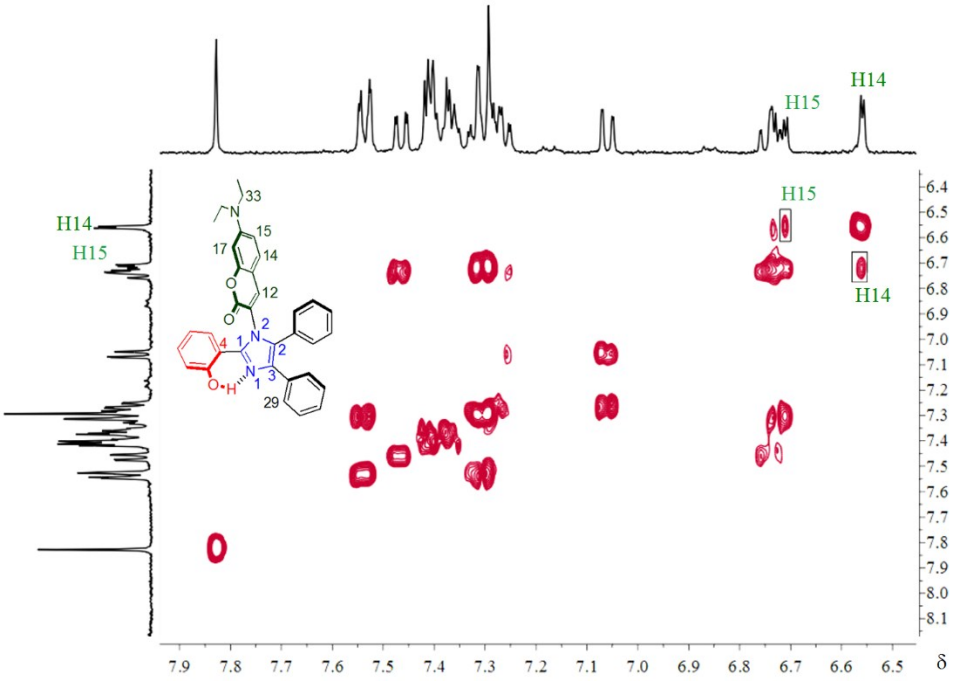

Fig. S13 2D COSEY spectrum (400 MHz, CD_3CN, 273 K) of compound **1**.

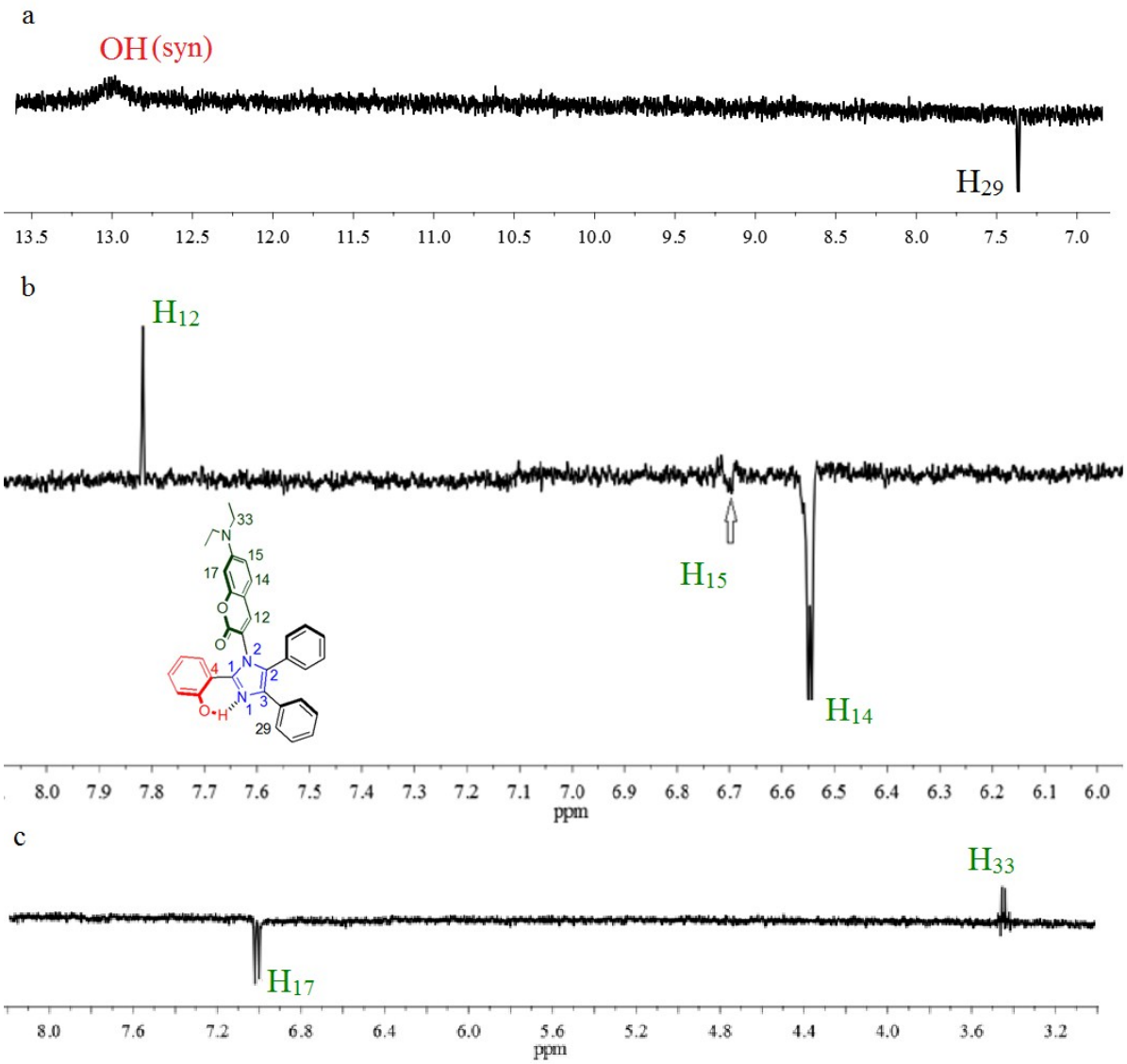

Fig. S14 1D NOESY spectra (400 MHz, CD_3CN, 273 K) of **1**; (a) Irradiation of H29, showing correlation with OH at 13.01 ppm (b) irradiation of proton H14 showing the correlation between H12 and COSY interaction with H15; and (c) irradiation of proton H17 showing the correlation between H33.

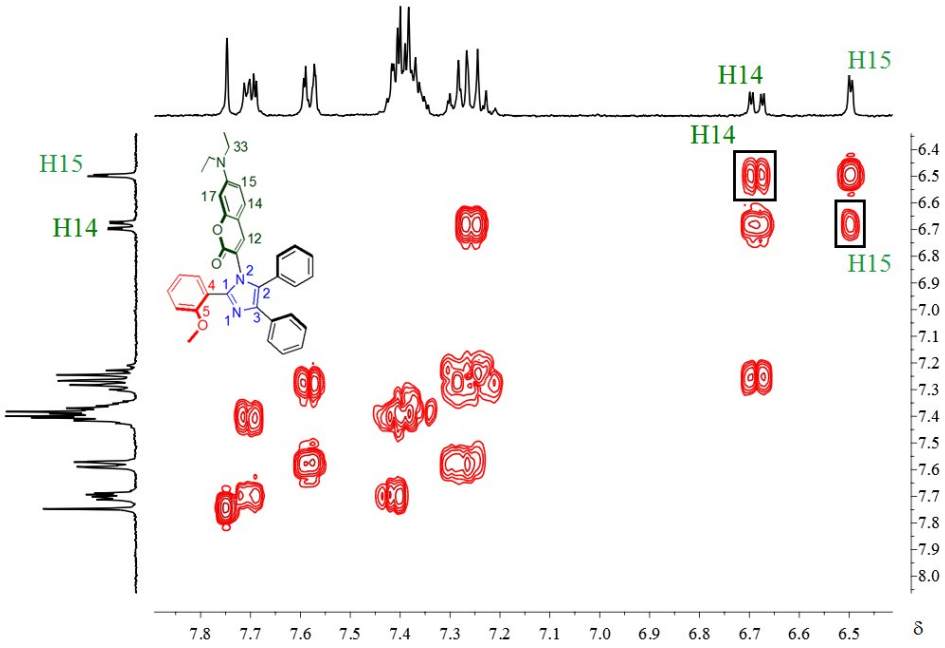

Fig. S15 2D COSEY spectrum (400 MHz, CD_3CN, 273 K) of compound **2.**

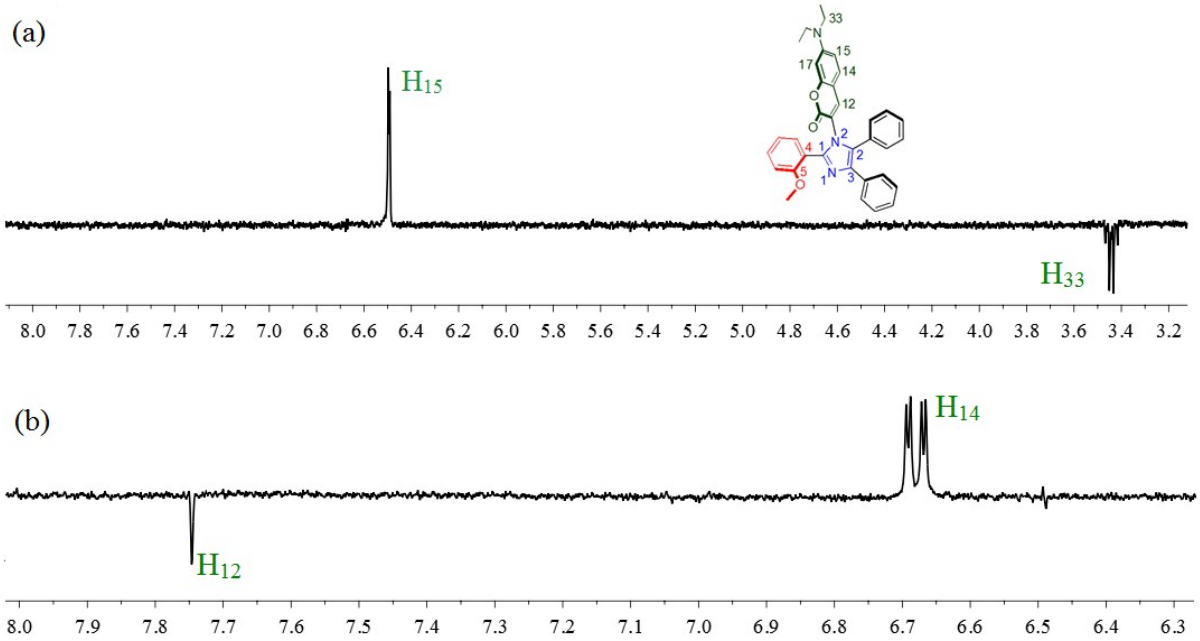

Fig. S16 1D NOESY spectra (400 MHz, CD_3CN, 308 K) of **2**; (a) irradiation of proton H15 showing the correlation between H33/31; and (b) irradiation of proton H12 showing the correlation between H12.

Rotational Barrier studies via VT NMR

Rotational barrier of 1 was calculated from variable temperature 1H NMR (on a Bruker 400 MHz spectrometer) by monitoring the coumarin proton (H12). Spectra were collected in CD_3CN at 2-3 K intervals within the range of 273 K to 283 K. Each peak were analyzed and integrate to plot Van't Hoff equation to calculate energy parameters of $\Delta G^{\#}$, $\Delta H^{\#}$ and $\Delta S^{\#}$. The equilibrium ratio was 90:10 (cis/trans) at 273 K, which decreases gradually with increase of temperature. At 283 K, this ratio becomes 56:44 (cis/trans). No significant change in equilibrium ratio was observed after 283 K and bellow 273K. The free energy change associated with this process (cis/trans) was calculated to be $\Delta G^{\#}$ = 0.5 kcal/mol at RT, which closely matches with the computational results ($\Delta G^{\#}$ = 0.69 kcal/mol). We could not extend the rate constant measurement studies in CD3CN because of low free energy of activation energy. In order to reach a better conclusion about the mechanism, one has to look at the full analysis of NMR.

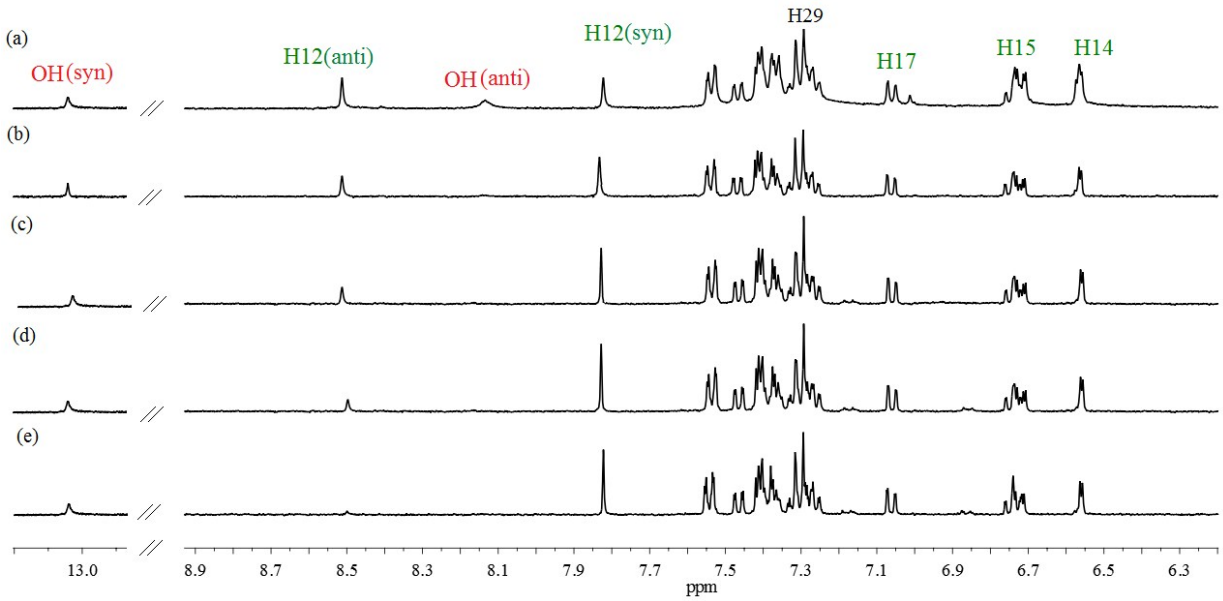

Fig. S17 Temperature dependent study of **1** in CD_3CN, (a) 283 K; (b) 280 K; (c) 278 K; (d) 276 K; (e) 273 K, clearly indicates formation of another rotamer with increasing temperature.

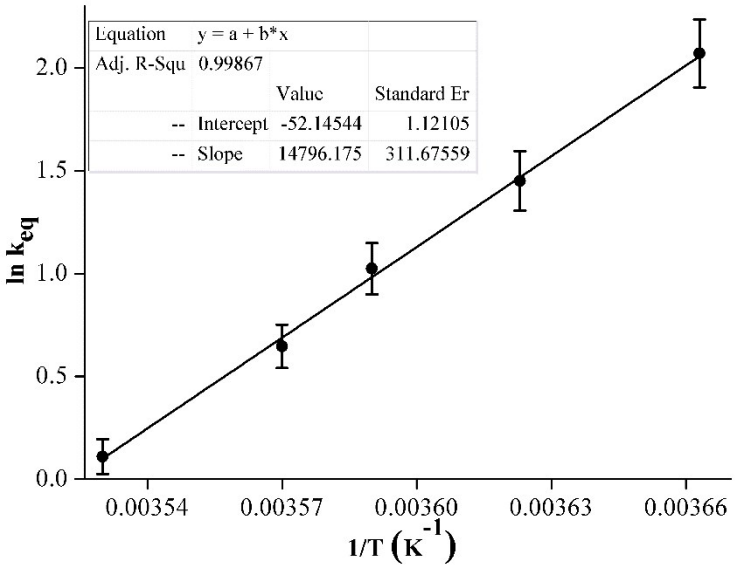

Fig. S18 Van't Hoff plot of equilibrium constant vs. 1/T. The free energy change at 283 K ($\Delta G^{\#}$ = – 0.1 kcal mol^{-1}) was calculated from the slope ($\Delta H^{\#}$ = – 29.3 kcal mol^{-1}) and intercept ($\Delta S^{\#}$ = – 103 cal K^{-1} mol^{-1}).

Single Crystal X-ray Diffraction (SCXRD) Analysis:

Synthesis of crystal 1. Compound **1** (0.5 g) was dissolved in 2 mL of toluene, and the resulting solution was diffused with hexane (2 mL). The mixture was allowed to evaporate slowly to produce cubic-shaped yellow crystals suitable for X-ray diffraction.

Synthesis of crystal 3: Compound **3** (0.75 g) was dissolved in 3 mL of ethyl acetate, and the resulting solution was diffused with hexane (2 mL). The mixture was allowed to evaporate slowly to produce rod-shaped yellow crystals suitable for X-ray diffraction.

X-ray diffractometer details: Single crystal X-ray diffraction was performed using a Bruker D8 Venture diffractometer operating with Mo Kα radiation and equipped with a Photon100 area detector. Single crystals were mounted at room temperature on the ends of glass fibers and data were collected at room temperature. Data collection: APEX2 (Bruker, 2014)[S2] cell refinement: SAINT (Bruker, 2014)[S2] data reduction: SAINT; program(s) used to solve structure: SHELXT (Sheldrick, 2008)[S3] program(s) used to refine structure: SHELXL2014 (Sheldrick, 2008); molecular graphics: Ortep-3 for Windows[S4].

1. The crystal structure of **1** (Figure S19) shows that there is an intramolecular H-bond (O–H•••N, 1.895 Aº, 147.3º) between the imidazolyl nitrogen (N1) and the hydroxyl OH proton. The

measured dihedral angles indicate that the phenyl (attached to C2 and C3 carbon atoms of imidazolyl ring), coumarin (attached to N2), hydroxyl phenyl (attached to C1) and imidazolyl rings deviate from planarity 67.2(4)^{o} (phenyl ring attached to C2), 6.6(5)^{o} (phenyl ring attached to C3), -92.1(1)^{o} (coumarin ring attached to N2) and 24.5(4)^{o} (attached to C1) when viewed along the N(2)-C(2)-C(19)-C(20) atoms, N(1)–C(3)–C(30)–C(29) atoms, the C(2)–N(2)–C(10)–C(12) atoms and N(1)–C(1)–C(4)–C(5) respectively. Moreover, the crystal structure of **1** indicates that the O1 atom from coumarin group is intermolecularly hydrogen bonded with atom H12 from coumarin of another molecule (C12–H···O1, 2.381 Å, 153.63º). In addition to this, hydroxyphenyl groups of two molecules are involved in π-π (face to face) interaction (3.748 Å). Moreover, an additional intermolecular C–H···C interactions between atoms of C5 and H21 (C23–H···C5, 2.9 Å, 126.71°), is also present in the crystal lattice. Thus, **1** prefers to pack in a face-to-face orientation, as seen along the b-axis.

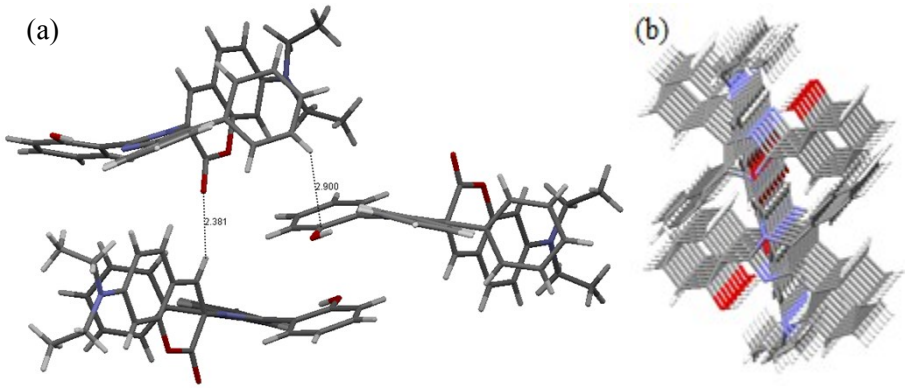

Fig. S19 (a) Intermolecular interaction and (b) crystal packing of **1**, viewed along b-axis.

3. The measured dihedral angles indicate that the phenyl (attached to C2 and C3 carbon atoms of imidazolyl ring), coumarin (attached to N2), hydroxyl phenyl (attached to C1) and imidazolyl rings deviate from planarity 76.1(3)^{o} (phenyl ring attached to C2), 21.9(3)^{o} (phenyl ring attached to C3), -83.3(3)^{o} (coumarin ring attached to N2) and -27.0(3)^{o} (attached to C1) when viewed along the N(2)-C(2)-C(19)-C(20) atoms, N(1)–C(3)–C(30)–C(29) atoms, the C(2)–N(2)–C(10)–C(12) atoms and N(1)–C(1)–C(4)–C(5) respectively. It is clear that the orientation of phenyl and coumarin peripheryl groups attached to C1, C2, C3 and N2 atoms of imidazolyl ring are significantly affected due to absence of intramolecular hydrogen bonding interaction.

Additionally, **3** shows two intermolecular hydrogen bond between atoms of N1 and H20 from two neighboring molecules (C20–H20···N1, 2.656 Å, 145.9°) and O1 and H31B (C31–H31B···O1, 2.347 Å, 143.1°). Moreover, two C–H···C interactions between atoms of C26 and H9 (C9–H9···C26, 2.891 Å, 132.6°), and C14 and H7 of adjacent molecule (C7–H7···C14, 2.835 Å, 160.26 °) , respectively are also present in the crystal lattice. Thus, the **3** prefers to pack in head to tail fashion, as viewed along a-axis.

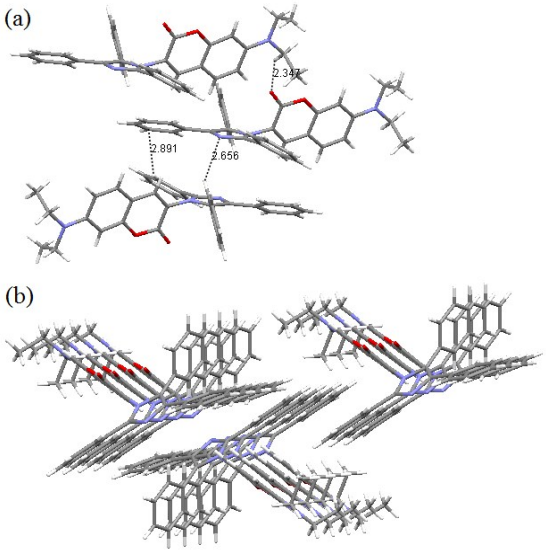

Fig. S20 (a) intermolecular interaction and (b) crystal packing of **3** viewed along a-axis.

Table S1.Crystal data and parameters of **1** and **3**.

	1	**3**
CCDC	1567243	1567244
Empirical formula	C34 H29 N3 O3	C34 H29 N3 O2
Formula weight	527.60	511.60
Temperature	297(2)	297(2)
Crystal system	monoclinic	Triclinic
Space Group	P 2_1/n	P -1
Unit cell dimensions	*a* = 14.0571(5) Å *b* =13.2680(5) Å, *c* = 15.3305(5) Å α = 90 ° β = 104.96(10)° γ = 90 °	*a* = 9.8322(6) Å *b* = 11.6973(7) Å *c* = 12.9750(7) Å α = 113.245(2) ° β = 93.220(2) ° γ = 93.119(2) °
Volume	2762.32(17) Å^3	1364.18(14) Å^3
Z	4	2
Density(calculated)	1.269 Mg/m^3	1.245 Mg/m^3
Absorption coefficient	0.082 mm^{-1}	0.078 mm^{-1}
F(000)	1112	594

Crystal size	0.344 × 0.328 × 0.265 mm^3	0.174 × 0.139 × 0.034 mm^3
Theta range for data collection	2.97 to 24.994 °	2.97 to 25.681 °
Index ranges	-16<=h<=16, -15<=k<=15, -18<=l<=18	-11<=h<=11, -14<=k<=14, -15<=l<=15
Reflections collected	49739	41215
Independent reflection	4848	5179
Completeness to θ	99.8%	99.9 %
Absorption correction	Multi-Scan	Multi-Scan
Max. and min. transmission	0.979 and 0.972	0.996 and 0.979
Refinement method	SHELXL-2014/7 (Sheldrick, 2014)	SHELXL-2014/7 (Sheldrick, 2014)
Data / restraints / parameters	4848 / 0 / 353	5179 / 0 / 355
Goodness-of-fit on F2	1.062	1.218
Final R indices [I>2σ(I)]	R = 0.0784 wR2 = 0.2266	R = 0.0565 wR2 = 0.1139
R indices(all data)	R = 0.1039 wR2 = 0.2532	R = 0.1252 wR2 = 0.1332
Largest diff. peak and hole	1.240 and -0.752 e.$Å^{-3}$	0.146 and -0.157 e.$Å^{-3}$

The IUCR's Check CIF routine indicated three B-level alert for **1**, generates from residual density, Hirshfeld test of N3 with C31 and C33 atom, which are due to thermal motion and a short distance is also found between C33 and C34.

Photophysical property

Absorption study of these compounds were carried out using ~10^{-5} M and steady state emission was measured at ~10^{-6} M concentration, unless otherwise specified.

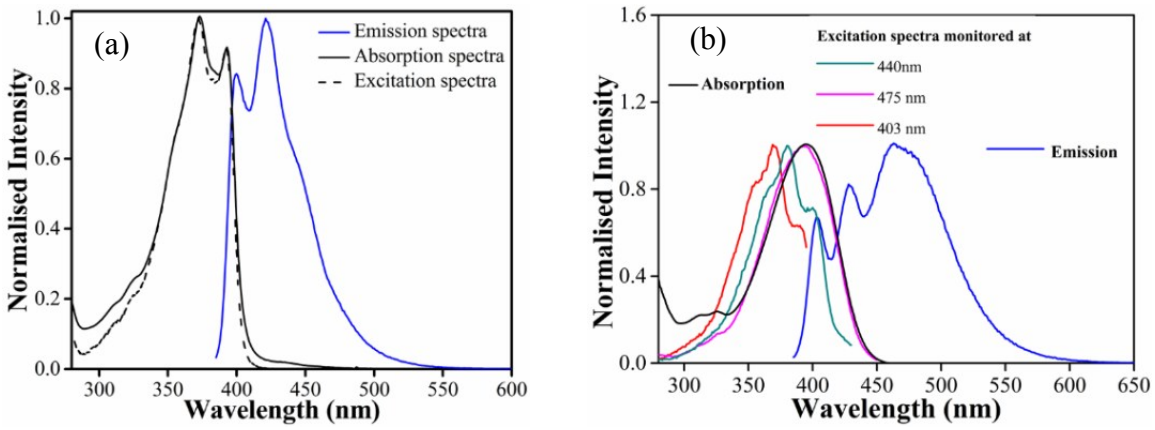

Fig. S21 Absorption, emission (excited at 375 nm) and excitation spectra (monitored at 403, 440 and 475 nm) of **1** in (a) cyclohexane and (b) EtOH.

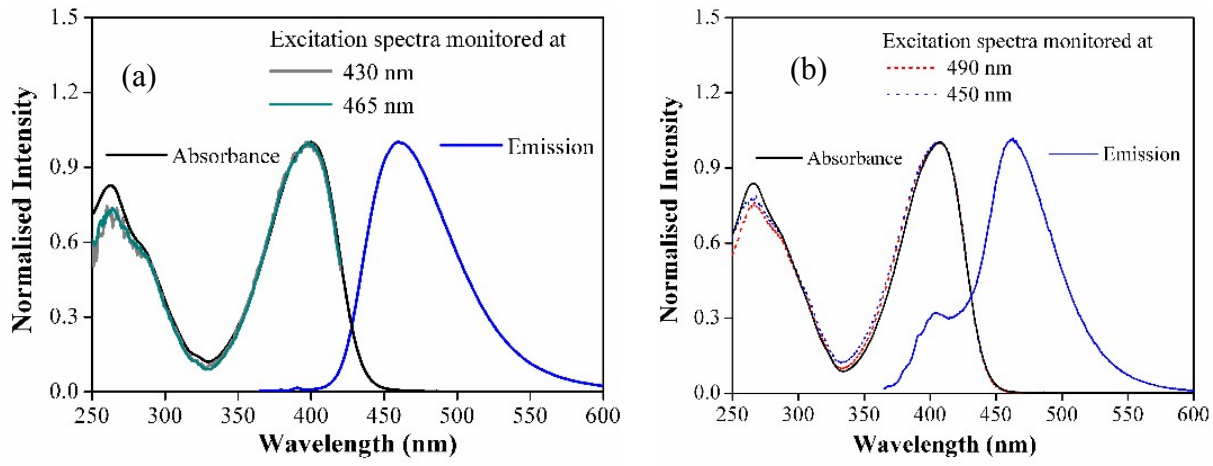

Fig. S22 Absorption, emission (excited at 375 nm) and excitation spectra of (a) **2** and (b) **3**, in Acetonitrile.

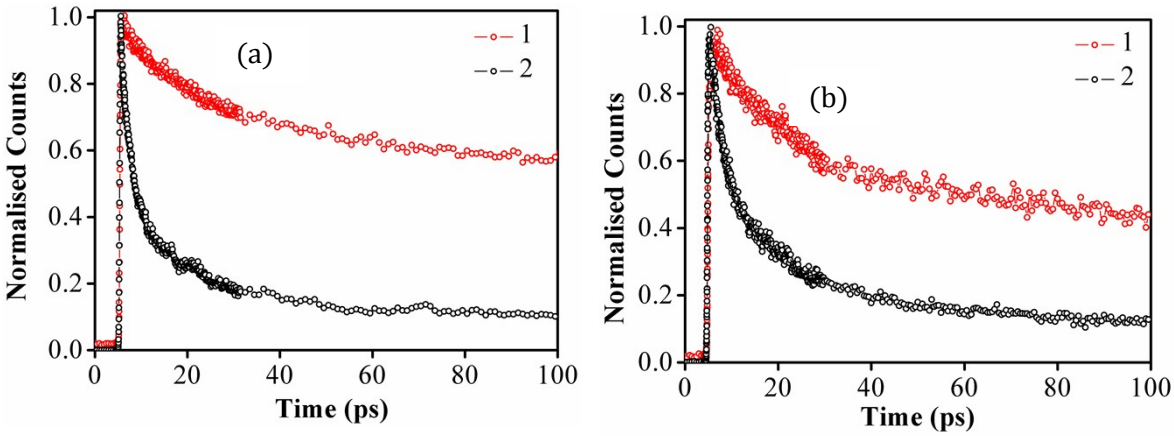

Fig. S23 Fluorescence upconversion decay of **1** & **2** in Acetonitrile (a) 475 nm; (b) 538 nm.

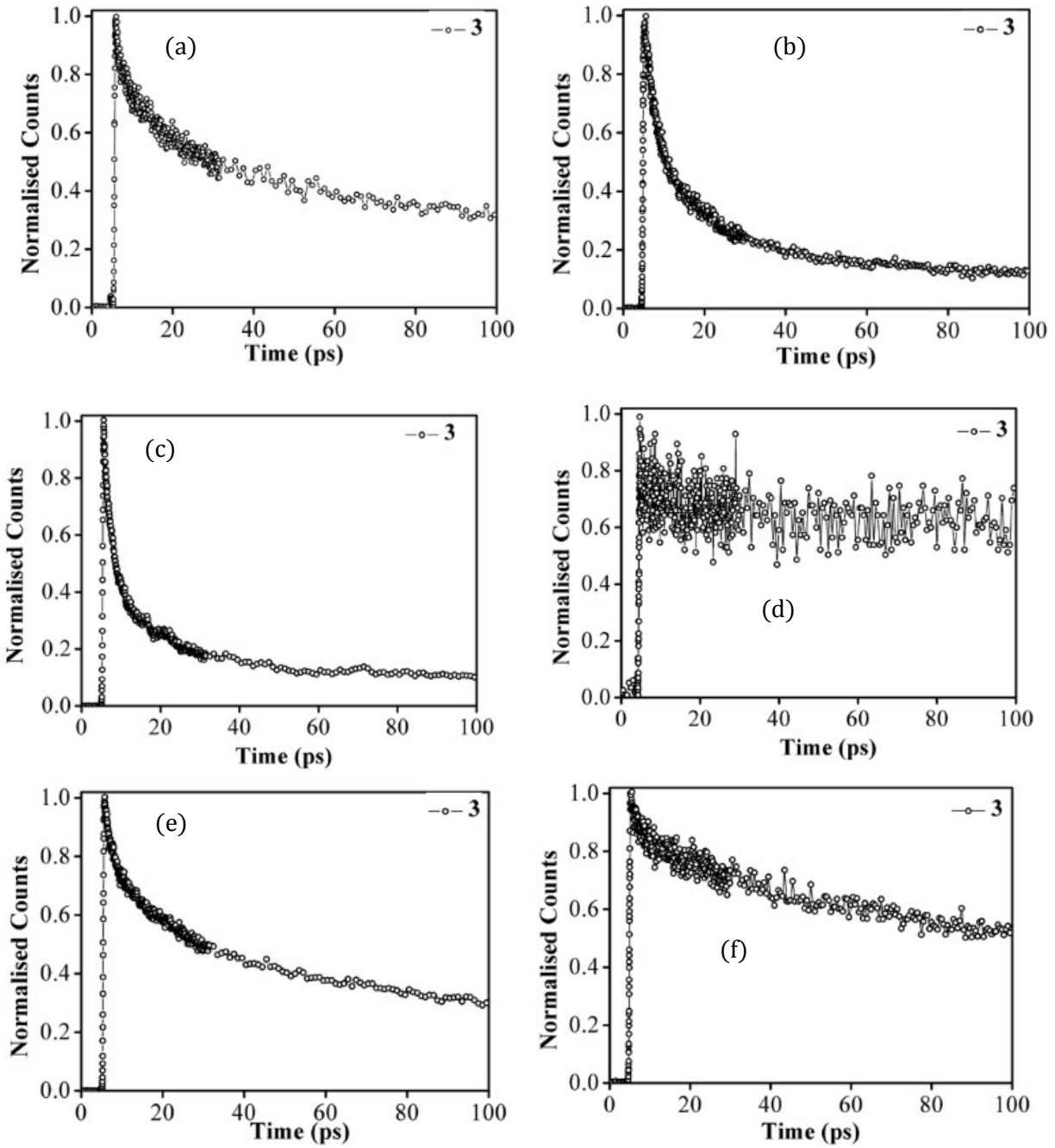

Fig. S24 Fluorescence upconversion decay of **3** in Acetonitrile (a) 475 nm; (b) 538 nm; Ethylene glycol (c) 475 nm; (d) 538 nm; and Ethanol (e) 475 nm; (f) 538 nm.

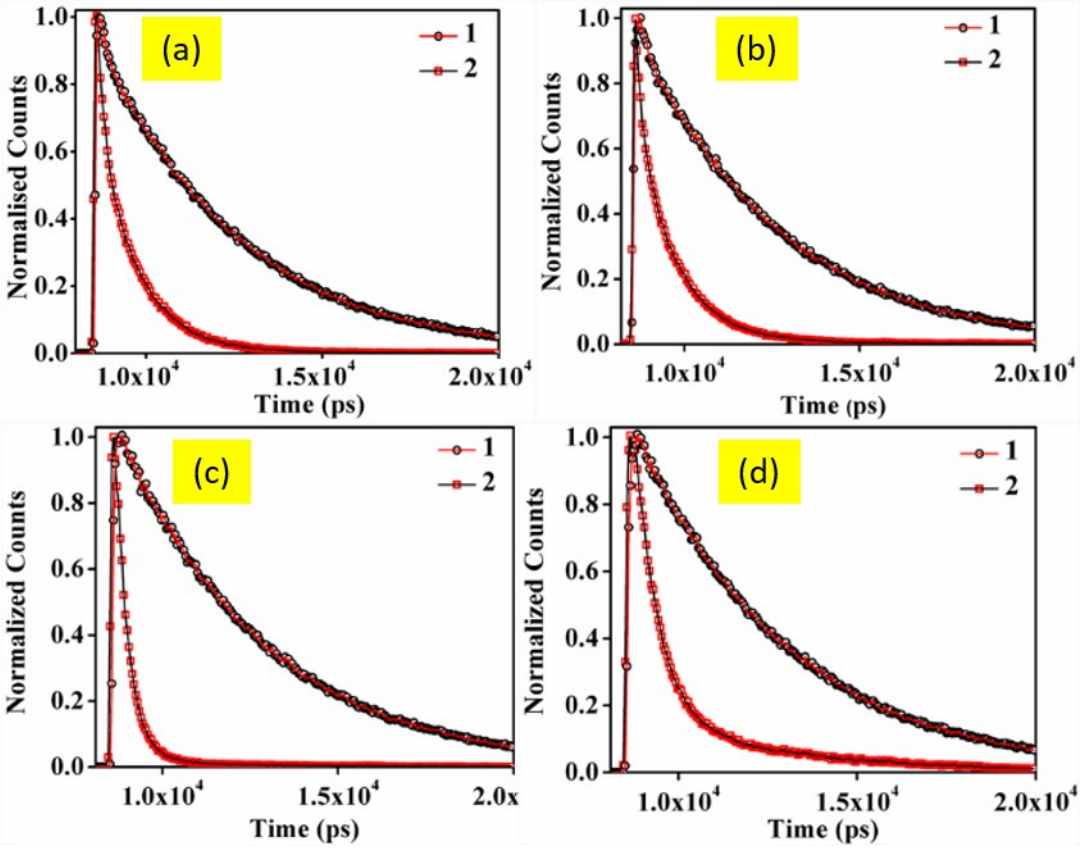

Fig. S25 Fluorescence TCSPC decay of **1** & **2** in Acetonitrile (a) 475 nm; (b) 538 nm; Ethanol (c) 538 nm; and Ethylene glycol (d) 538 nm.

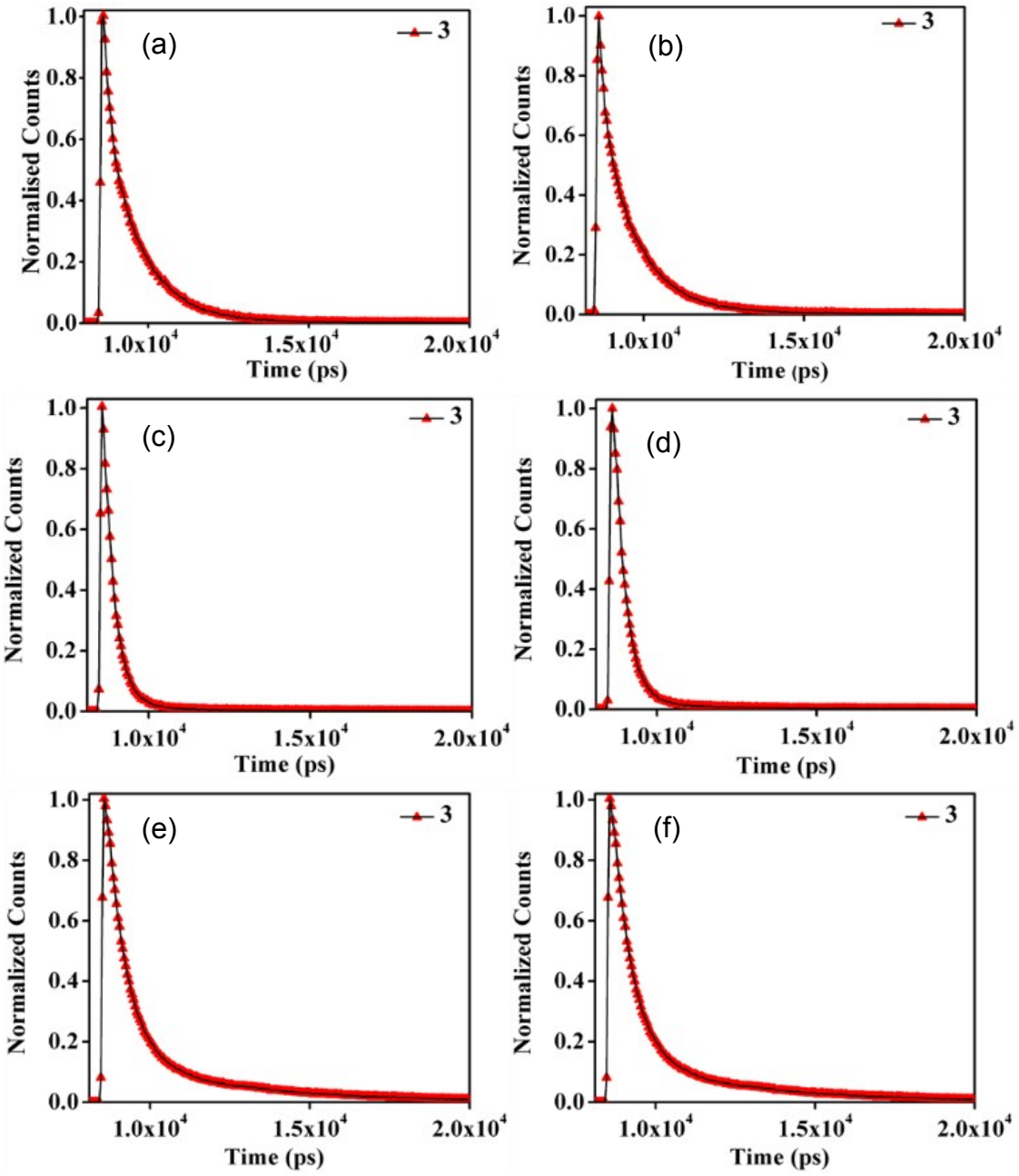

Fig. S26 Fluorescence TCSPC decay of **3** in Acetonitrile (a) 475 nm; (b) 538 nm; Ethanol (c) 475 nm; (d) 538 nm; and Ethylene glycol (e) 475 nm; (f) 538 nm.

Theoretical Calculation. The initial geometry of the ground (S_0) and first singlet excited state (S_1) of **1**, **2** and **3** were optimized using density functional theory (DFT for S_0) and time-dependent density functional theory (TDDFT for S_1).[S5] Vertical excitation energies at the ground state geometries were calculated using TDDFT with different functionals (B3LYP, CAM-B3LYP, M06-2X).[S6-S11] All the calculations has been enumerated using 6-311G(d,p) basis set. The DFT and TDDFT calculations were carried out using Gaussian 09, Revision D.01 package.[S12] Moreover, solvent plays a crucial role on the potential energy barrier of isomerization process. Therefore, the solvent effect has been considered in self-consistent reaction field method (SCRF)[S13,S14] to calculate the optimized geometry of **1, 2,** and **3** respectively. First, all the compound has been optimized (B3LYP/6-311G(d,p)) by SCRF model using ethanol as a solvent. All the compounds has been optimized by using different functional using same 6-311G(d,p) basis set.

Table S2: Optimized geometry and their corresponding energy of **1**, **2**, and **3** using different functional.

Compounds	B3LYP	CAM-B3LYP	M06-2X
1	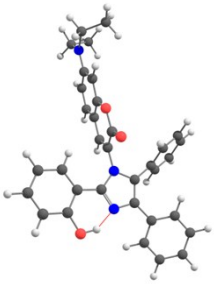	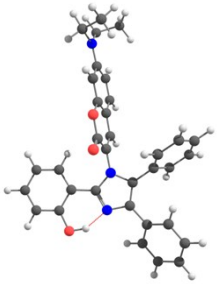	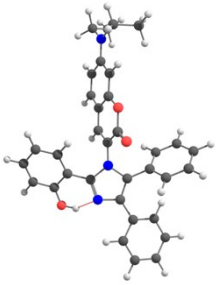
	-1703.48054 (au)	-1702.58819 (au)	-1702.79855 (au)
2	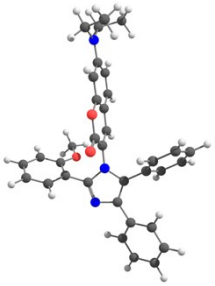	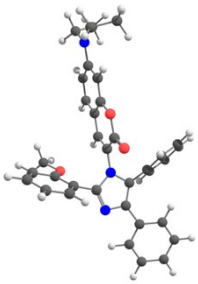	
	-1742.77856 (au)	-1741.85925 (au)	

3	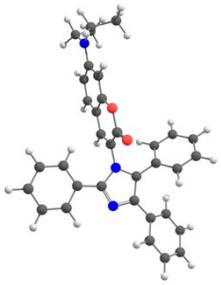	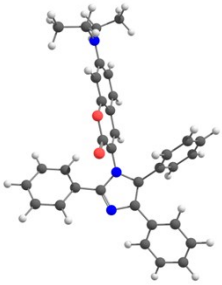	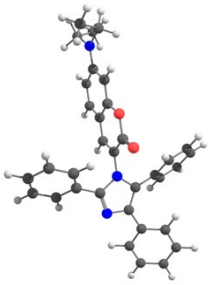
	-1628.20773 (au)	-1627.35003 (au)	-1627.56927 (au)

Table S3: Comparison between the H-bond distances, angles, and torsions between cis, trans and crystal geometry of **1**.

	Hydrogen Bond		Torsion (°)			
	Distance (Å)	Angle (°)	N2–C2–C19–C20	N1–C3–C30–C29	C2–N2–C10–C12	N1–C1–C4–C5
crystal	1.890(1) [a]	148.06(0) [a]	66.87(0)	6.39(0)	-92.01(0)	24.77(0)
cis	1.65 [a]	148.62 [a]	65.48	28.1	81.85	0.13
trans	1.84 [b]	153.4 [b]	63.36	24.38	79.58	96.33

[a]H-bond between O3–H3•••N1; [b]H-bond between O3–H3•••O1.

Natural Bonding orbital (NBO) analysis. NBO analysis has been carried out using B3LYP/6-311G(d,p) level of theory. In compound **1**, two isomers were found in PES scan, to find out additional stability, we performed NBO calculation[S15]. This additional stability mainly arise due the spatial interaction between the lone pair of electron and anti-bonding orbitals. In both of the cases (cis or trans), NBO interaction was found. In table S4, it is clear that cis is having only one interaction, whereas, trans is stabilised due to four interactions between lone pair of electrons and σ^* and/or π^* orbital.

Table S4: NBO interactions of trans.

anti			syn		
Donor – Acceptor	Orbital Interaction	E^2 (kcal/mol)	Donor – Acceptor	Orbital Interaction	E^2 (kcal/mol)
$n_{P_x\,(O3)} - \pi^*_{CN}$	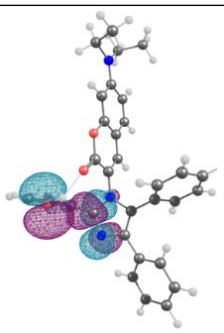	0.18	$n_{P_x\,(O3)} - \sigma^*_{CN}$	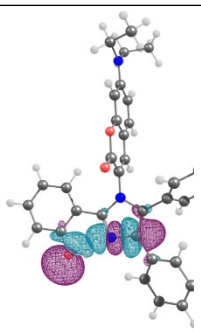	1.26
$n_{P_x\,(O3)} - \pi^*_{CO}$	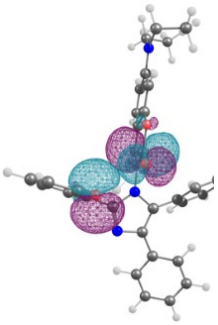	0.11			
$n_{P_x\,(O1)} - \sigma^*_{OH}$	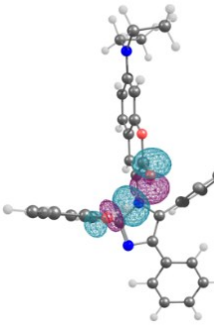	5.13			
$n_{P_y\,(O1)} - \sigma^*_{OH}$	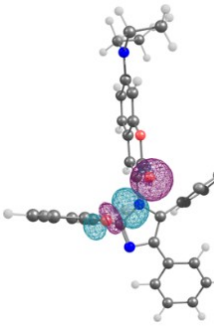	3.59			

Frontier Orbitals Analysis

Table S5: The calculated (B3LYP/6-311G(d,p)) molecular orbital energy levels, transition energies and oscillator strengths of the syn conformer of **1**.

Transition	Energy (eV)	Energy (nm)	Oscillator Strength (f)
HOMO to LUMO	3.01	411.29	0.12
HOMO - 1 to LUMO	3.19	388.52	0.765
HOMO - 2 to LUMO	3.78	327.57	0.0023
HOMO to LUMO + 1	3.89	318.27	0.70
HOMO - 1 to LUMO + 1	4.02	307.81	0.0503
HOMO to LUMO + 2	4.14	299.34	0.2474

Table S6: The calculated (B3LYP/6-311G(d,p)) molecular orbital energy levels, transition energies and oscillator strengths of the anti conformer of **1.**

Transition	Energy (eV)	Energy (nm)	Oscillator Strength (f)
HOMO to LUMO	3.1	399.77	0.8754
HOMO - 2 to LUMO	3.63	341.11	0.0139
HOMO - 1 to LUMO + 1	4.15	298.3	0.3925

Table S7: The calculated (B3LYP/6-311G(d,p)) molecular orbital energy levels, transition energies and oscillator strengths of the **2**.

Transition	Energy (eV)	Energy (nm)	Oscillator Strength (f)
HOMO to LUMO	3.22	384.94	0.8971
HOMO - 3 to LUMO	3.808	325.86	0.0136
HOMO - 2 to LUMO + 1	4.15	298.45	0.3467

Table S8: The calculated (B3LYP/6-311G(d,p)) molecular orbital energy levels, transition energies and oscillator strengths of the **3**.

Transition	Energy (eV)	Energy (nm)	Oscillator Strength (f)
HOMO to LUMO	3.03	408.47	0.1251
HOMO - 1 to LUMO	3.169	391.17	0.7922
HOMO to LUMO + 1	3.98	311.3	0.2638
HOMO -1 to LUMO + 1	4.086	303.41	0.2145
HOMO -1 to LUMO + 2	4.15	298.72	0.5329

Compound	HOMO-1	HOMO	LUMO
2		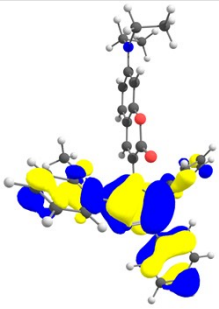	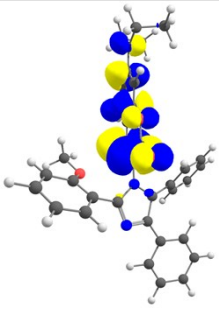
3	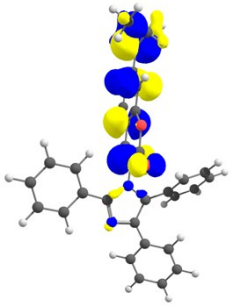	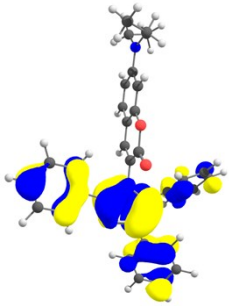	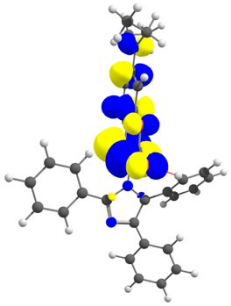

Fig. S27 The calculated (B3LYP/6-311G(d,p)) molecular orbital contour surfaces of **2** and **3**.

Optimized coordinate of syn:

	X	Y	Z
7	-3.444990000	1.047174000	-0.137586000
6	-3.433872000	-0.326359000	-0.078361000
6	-2.127807000	-0.759151000	0.022868000
7	-1.340004000	0.399173000	0.026087000
6	-2.193254000	1.481639000	-0.068970000
6	-1.876979000	2.914947000	-0.087113000
6	-2.956951000	3.847382000	-0.084891000
6	-2.689105000	5.222271000	-0.087977000
6	-1.386807000	5.697564000	-0.103802000
6	-0.318190000	4.799265000	-0.117151000
6	-0.569351000	3.434613000	-0.109345000
8	-4.251656000	3.475503000	-0.074545000
1	-4.273942000	2.477402000	-0.089948000
6	-4.693025000	-1.088521000	-0.124555000
6	-5.802644000	-0.548546000	-0.794470000
6	-7.011479000	-1.236671000	-0.840919000
6	-7.138607000	-2.477900000	-0.217926000
6	-6.045457000	-3.021165000	0.456428000
6	-4.835539000	-2.334100000	0.506467000
6	-1.549217000	-2.116382000	0.079567000
6	-0.851550000	-2.558348000	1.212886000
6	-0.324623000	-3.846725000	1.259139000
6	-0.491296000	-4.712005000	0.178314000
6	-1.186830000	-4.282546000	-0.951164000
6	-1.710112000	-2.992760000	-1.002252000
6	0.084747000	0.383076000	0.124771000
6	0.875467000	0.160593000	-0.962924000

6	2.286312000	0.117576000	-0.838974000
6	0.651536000	0.544588000	1.451892000
8	2.035850000	0.511891000	1.526060000
8	0.039308000	0.700612000	2.484025000
6	2.847505000	0.303770000	0.440277000
6	3.186755000	-0.101958000	-1.903542000
6	4.544730000	-0.127551000	-1.702673000
6	5.109444000	0.077469000	-0.403161000
6	4.208385000	0.282476000	0.670796000
7	6.461501000	0.086363000	-0.209020000
6	7.398359000	-0.138697000	-1.319054000
6	7.034668000	0.281844000	1.129723000
6	7.073855000	-0.979207000	2.000737000
6	7.631472000	-1.612162000	-1.671239000
1	7.704970000	-1.748930000	1.552206000
1	7.485531000	-0.733392000	2.983369000
1	6.076677000	-1.399451000	2.147349000
1	8.048067000	0.659827000	0.989397000
1	6.483425000	1.076470000	1.638579000
1	8.320701000	-1.683253000	-2.517118000
1	8.070015000	-2.153775000	-0.830742000
1	6.700965000	-2.111679000	-1.949607000
1	8.344580000	0.321763000	-1.031953000
1	7.050426000	0.410890000	-2.196441000
1	4.546493000	0.422144000	1.685766000
1	5.186562000	-0.309037000	-2.551042000
1	2.790466000	-0.256576000	-2.900696000
1	0.419739000	0.023051000	-1.937490000
1	-0.736429000	-1.895430000	2.062350000

1	0.209954000	-4.176424000	2.142646000
1	-0.083145000	-5.715470000	0.216966000
1	-1.318839000	-4.949761000	-1.795267000
1	-2.245837000	-2.658348000	-1.882903000
1	-4.002795000	-2.760449000	1.051074000
1	-6.136346000	-3.979938000	0.954636000
1	-8.080153000	-3.013936000	-0.253696000
1	-7.854955000	-0.803538000	-1.366981000
1	-5.706967000	0.413068000	-1.283864000
1	0.270740000	2.758928000	-0.132758000
1	0.703766000	5.157681000	-0.135742000
1	-1.204915000	6.766335000	-0.108235000
1	-3.535589000	5.898898000	-0.080946000

Optimized coordinate of anti:

	X	Y	Z
7	-3.472936000	1.233282000	-0.268035000
6	-3.552134000	-0.142346000	-0.156348000
6	-2.283541000	-0.674610000	-0.008948000
7	-1.422224000	0.425085000	-0.027644000
6	-2.202397000	1.552758000	-0.181275000
6	-1.675549000	2.935699000	-0.276056000
6	-1.401666000	3.702474000	0.873342000
6	-1.035154000	5.045812000	0.736071000
6	-0.925385000	5.624029000	-0.522578000
6	-1.175933000	4.868731000	-1.668946000
6	-1.552357000	3.536753000	-1.535821000
8	-1.528684000	3.219403000	2.140693000
1	-1.262339000	2.281721000	2.190465000

6	-4.864682000	-0.811521000	-0.193276000
6	-5.941397000	-0.176442000	-0.833623000
6	-7.198463000	-0.771600000	-0.878626000
6	-7.410971000	-2.014277000	-0.281850000
6	-6.353205000	-2.650061000	0.367460000
6	-5.094889000	-2.055506000	0.415786000
6	-1.788819000	-2.059868000	0.115968000
6	-1.109100000	-2.479863000	1.268572000
6	-0.646608000	-3.789008000	1.379453000
6	-0.859687000	-4.697827000	0.343624000
6	-1.536203000	-4.290403000	-0.805676000
6	-1.994374000	-2.980302000	-0.921040000
6	-0.000576000	0.378496000	0.055369000
6	0.782271000	0.077063000	-1.021769000
6	2.189493000	-0.003039000	-0.893763000
6	0.585078000	0.634812000	1.350246000
8	1.951618000	0.542207000	1.442490000
8	-0.024090000	0.925295000	2.368532000
6	2.757428000	0.231636000	0.374584000
6	3.083852000	-0.317128000	-1.940642000
6	4.438039000	-0.389783000	-1.730418000
6	5.008040000	-0.140999000	-0.440078000
6	4.113721000	0.163578000	0.616039000
7	6.357127000	-0.184945000	-0.238728000
6	7.287249000	-0.506725000	-1.331239000
6	6.933920000	0.046554000	1.093233000
6	6.900130000	-1.170242000	2.025056000
6	7.457700000	-2.004886000	-1.606102000
1	7.489868000	-1.994244000	1.618788000

1	7.320478000	-0.899078000	2.997236000
1	5.880848000	-1.527862000	2.185203000
1	7.966873000	0.361541000	0.941379000
1	6.424388000	0.894408000	1.557574000
1	8.146336000	-2.148248000	-2.443196000
1	7.869574000	-2.521405000	-0.736903000
1	6.507511000	-2.477312000	-1.864417000
1	8.251140000	-0.072687000	-1.062692000
1	6.965763000	0.011439000	-2.237174000
1	4.454008000	0.346962000	1.623220000
1	5.074268000	-0.645073000	-2.563865000
1	2.684731000	-0.509774000	-2.929950000
1	0.319740000	-0.110993000	-1.984391000
1	-0.956911000	-1.781820000	2.083815000
1	-0.125301000	-4.099997000	2.277601000
1	-0.501424000	-5.717107000	0.431752000
1	-1.702691000	-4.991137000	-1.615916000
1	-2.513540000	-2.663561000	-1.818043000
1	-4.291492000	-2.555612000	0.941134000
1	-6.509024000	-3.609906000	0.847545000
1	-8.389899000	-2.478766000	-0.316870000
1	-8.014015000	-0.264318000	-1.382342000
1	-5.778327000	0.790794000	-1.291912000
1	-1.773894000	2.944402000	-2.416358000
1	-1.088705000	5.314400000	-2.652474000
1	-0.637645000	6.665833000	-0.608299000
1	-0.837832000	5.616464000	1.635850000

Optimized coordinate of 2:

	X	Y	Z
7	3.442072000	1.301942000	-0.152185000
6	2.147824000	1.518958000	-0.200233000
7	1.445233000	0.336470000	-0.143350000
6	2.380357000	-0.695698000	-0.057483000
6	3.613736000	-0.067889000	-0.065024000
6	1.513006000	2.847774000	-0.340842000
6	0.769955000	3.421607000	0.712396000
6	0.211976000	4.694086000	0.557029000
6	0.404101000	5.398139000	-0.631612000
6	1.150011000	4.850365000	-1.670242000
6	1.699942000	3.579323000	-1.514967000
8	0.663754000	2.676482000	1.846264000
6	-0.026118000	3.227939000	2.970293000
1	-1.077460000	3.419455000	2.737556000
1	0.040392000	2.475661000	3.753477000
1	0.450500000	4.151369000	3.311165000
1	-0.360108000	5.145345000	1.355766000
1	-0.033364000	6.384658000	-0.735657000
1	1.301715000	5.401207000	-2.590500000
1	2.282067000	3.134602000	-2.313334000
6	0.031235000	0.200454000	-0.257671000
6	-0.770614000	0.058109000	0.833398000
6	-2.176369000	-0.070653000	0.691753000
6	-2.719451000	-0.039720000	-0.607239000
8	-1.897511000	0.098335000	-1.695513000
6	-0.517398000	0.208820000	-1.601946000
8	0.105136000	0.293711000	-2.637126000

6	-4.074019000	-0.149570000	-0.855387000
6	-4.986124000	-0.289468000	0.218857000
6	-4.438732000	-0.339830000	1.539951000
6	-3.086815000	-0.228279000	1.757884000
1	-0.328365000	0.049013000	1.822186000
1	-2.704159000	-0.265747000	2.771625000
1	-5.087942000	-0.469280000	2.392222000
1	-4.397533000	-0.128235000	-1.884460000
7	-6.334604000	-0.361563000	0.004233000
6	-7.280363000	-0.527114000	1.116556000
6	-6.890547000	-0.309572000	-1.354365000
6	-6.874603000	-1.645916000	-2.105808000
6	-7.443110000	-1.969176000	1.610417000
1	-7.276399000	-1.506141000	-3.113089000
1	-7.488552000	-2.391617000	-1.596765000
1	-5.861838000	-2.043842000	-2.197810000
1	-7.831621000	-2.615248000	0.820642000
1	-6.494288000	-2.386409000	1.954616000
1	-8.147456000	-1.994418000	2.446460000
1	-7.917825000	0.046193000	-1.264641000
1	-6.356075000	0.452300000	-1.927158000
1	-6.979807000	0.123576000	1.941156000
1	-8.243672000	-0.149494000	0.771198000
6	1.984086000	-2.114531000	0.051010000
6	2.272288000	-2.840543000	1.214936000
6	1.909673000	-4.181103000	1.321666000
6	1.248581000	-4.814151000	0.269654000
6	0.954535000	-4.100246000	-0.891498000
6	1.320566000	-2.760680000	-1.002034000

1	2.780768000	-2.348471000	2.035898000
1	2.139410000	-4.729495000	2.228236000
1	0.965114000	-5.857083000	0.353831000
1	0.444662000	-4.587177000	-1.715058000
1	1.105727000	-2.214121000	-1.912955000
6	4.970416000	-0.638624000	-0.001871000
6	5.261733000	-1.943436000	-0.431355000
6	6.561111000	-2.440573000	-0.369616000
6	7.600085000	-1.646024000	0.114223000
6	7.325959000	-0.343903000	0.532412000
6	6.027799000	0.154203000	0.474213000
1	5.815152000	1.166454000	0.794304000
1	4.472876000	-2.568665000	-0.829282000
1	6.763214000	-3.450101000	-0.710445000
1	8.611060000	-2.034880000	0.159445000
1	8.125597000	0.285969000	0.906766000

Optimized coordinate of 3:

	X	Y	Z
7	-3.412449000	1.471897000	-0.196403000
6	-3.610578000	0.152170000	-0.116324000
6	-2.339606000	-0.510709000	0.069865000
7	-1.416212000	0.485578000	0.125550000
6	-2.098206000	1.692495000	-0.050791000
6	-1.551303000	3.034751000	-0.075511000
6	-2.482382000	4.096996000	-0.182413000
6	-2.054862000	5.412341000	-0.207615000
6	-0.690351000	5.706692000	-0.129367000
6	0.239738000	4.671950000	-0.027042000

6	-0.175939000	3.347876000	0.000574000
1	-3.535278000	3.860295000	-0.236921000
1	-2.780599000	6.212572000	-0.286126000
1	-0.355489000	6.737082000	-0.149163000
1	1.297552000	4.897949000	0.029346000
1	0.555976000	2.560903000	0.066132000
6	0.009553000	0.282834000	0.225302000
6	0.771111000	0.180902000	-0.962944000
1	0.297383000	0.244197000	-1.932223000
6	2.175015000	0.000216000	-0.839334000
6	2.739513000	-0.063930000	0.458169000
8	1.951046000	0.056143000	1.589782000
6	0.542596000	0.221064000	1.517199000
8	-0.041798000	0.269704000	2.605441000
6	3.089583000	-0.128385000	-1.906229000
6	4.451291000	-0.307876000	-1.705289000
6	5.002214000	-0.365428000	-0.403452000
6	4.095061000	-0.235059000	0.677016000
7	6.362169000	-0.539735000	-0.185719000
6	6.907483000	-0.731156000	1.155280000
6	7.317783000	-0.561847000	-1.289425000
6	7.250161000	0.573812000	1.885720000
6	7.522059000	-1.947542000	-1.915608000
1	7.986728000	1.152546000	1.321780000
1	6.363552000	1.197064000	2.022462000
1	7.671597000	0.358682000	2.872162000
1	7.810258000	-1.340473000	1.060005000
1	6.210066000	-1.325373000	1.751270000
1	8.273167000	-0.194148000	-0.905205000

1	7.008460000	0.156313000	-2.053002000
1	6.590925000	-2.334615000	-2.335566000
1	7.878668000	-2.662069000	-1.168723000
1	8.264343000	-1.897680000	-2.717777000
1	4.429813000	-0.249725000	1.704337000
1	5.085910000	-0.417800000	-2.573333000
1	2.708973000	-0.094029000	-2.921884000
6	-4.948760000	-0.421960000	-0.176441000
6	-5.954251000	0.278700000	-0.871511000
6	-7.245561000	-0.222890000	-0.932130000
6	-7.563867000	-1.419920000	-0.284899000
6	-6.582190000	-2.111284000	0.424835000
6	-5.282515000	-1.622900000	0.478315000
1	-4.536392000	-2.154654000	1.052172000
1	-6.831247000	-3.029191000	0.943382000
1	-8.574654000	-1.807895000	-0.329570000
1	-8.007536000	0.315515000	-1.482833000
1	-5.699270000	1.205464000	-1.368488000
6	-2.033065000	-1.932767000	0.133875000
6	-1.233980000	-2.463476000	1.163179000
6	-0.967136000	-3.827120000	1.195289000
6	-1.466196000	-4.668259000	0.199860000
6	-2.255062000	-4.146916000	-0.826675000
6	-2.551041000	-2.790434000	-0.855246000
1	-3.158330000	-2.386094000	-1.655267000
1	-2.639756000	-4.796925000	-1.603113000
1	-1.244719000	-5.728772000	0.226127000
1	-0.367898000	-4.235349000	2.000326000
1	-0.868609000	-1.812389000	1.946520000

References:

S1. D. Ray and P. K. Bharadwaj, *Inorg. Chem.* 2008, **47**, 2252-2254.

S2. Bruker. APEX2, SAINT and SADABS. Bruker AXS Inc., Madison, Wisconsin, USA, 2014.

S3. G. M. Sheldrick, *Acta Cryst. Section* C. 2015, **71**, 3-8.

S4. L. J. Farrugia, *J. Appl. Cryst*. 1997, **30**, 565-565.

S5. E. Runge and E. K. U. Gross, *Phys. Rev. Lett*. 1984, **52**, 997-1000.

S6. A. D. Becke, *J. Chem. Phys*., 1993, **98**, 5648-5652.

S7. C. Lee, W. Yang and R. G. Parr, *Phys. Rev.* B, 1988, **37**, 785-789.

S8. S. H. Vosko, L. Wilk and M. Nusair, *Can. J. Phys*. 1980, **58**, 1200-1211.

S9. P. J. Stephens, F. J. Devlin, C. F. Chabalowski and M. J. Frisch, *J. Phys. Chem*., 1994, **98**, 11623-11627.

S10. Y. Takeshi, P. T. David and C. H. Nicholas *Chem. Phys. Lett*., 2004, **393**, 51-57.

S11. Y. Zhao and D. G. Truhlar, *Theor. Chem. Acc*., 2008, **120**, 215-241.

S12. M. J. Frisch, G. W. Trucks, H. B. Schlegel, G. E. Scuseria, M. A. Robb, J. R. Cheeseman, G. Scalmani, V. Barone, B. Mennucci, G. A. Petersson, H. Nakatsuji, M. Caricato, X. Li, H. P. Hratchian, A. F. Izmaylov, J. Bloino, G. Zheng, J. L. Sonnenberg, M. Hada, M. Ehara, K. Toyota, R. Fukuda, J. Hasegawa, M. Ishida, T. Nakajima, Y. Honda, O. Kitao, H. Nakai, T. Vreven, J. A. Mont-gomery, Jr., J. E. Peralta, F. Ogliaro, M. Bearpark, J. J. Heyd, E. Brothers, K. N. Kudin, V. N. Staroverov, T. Keith, R. Kobayashi, J. Normand, K. Raghavachari, A. Rendell, J. C. Burant, S. S. Iyengar, J. Tomasi, M. Cossi, N. Rega, J. M. Millam, M. Klene, J. E. Knox, J. B. Cross, V. Bakken, C. Adamo, J. Jaramillo, R. Gomperts, R. E. Stratmann, O. Yazyev, A. J. Austin, R. Cammi, C. Pomelli, J. W. Ochterski, R. L. Martin, K. Morokuma, V. G. Zakrzewski, G. A. Voth, P. Salvador, J. J. Dannenberg, S. Dap-prich, A. D. Daniels, O. Farkas, J. B. Foresman, J. V. Ortiz, J. Cioslowski and D. J. Fox, Gaussian, Inc., Wallingford CT, 2013.

S13. M. W. Wong, M. J. Frisch and K. B. Wiberg, *J. Am. Chem. Soc*. 1991, **113**, 4776-4782.

S14. M. W. Wong, K. B. Wiberg and M. J. Frisch, *J. Am. Chem. Soc*. 1992, **114**, 523-529.

S15. A. E. Reed and F. Weinhold, *J. Chem. Phys*. 1983, **78**, 4066-4073.